

# FOURIER ANALYSIS OF ORIENTATION HISTOGRAMS FOR TEXTURE CLASSIFICATION

M. ALEMÁN-FLORES and L. ÁLVAREZ-LEÓN

Departamento de Informática y Sistemas  
Universidad de Las Palmas de Gran Canaria  
Campus de Tafira, 35017, Las Palmas, SPAIN  
email: {maleman, lalvarez}@dis.ulpgc.es

## ABSTRACT

This work presents an approach to texture classification in which orientation histograms have been generated to compare textured regions. The orientation and magnitude of the gradient in every point of a texture are estimated and, combining them, an orientation histogram is built for each texture. Fourier analysis is used to measure the similarity of the histograms, considering the effects of a change in the size or orientation of the image. We have introduced a weighting function to reduce the influence of noise. Furthermore, we have tested the robustness of our method when some grayscale transformations are performed on the images.

## KEY WORDS

Image Processing and Analysis, Texture Analysis, Edge Orientation, Fourier Transform.

## 1. Introduction

The texture of a region may be helpful to a large extent when we try to characterize materials, components, agglomerations, etc. A texture can be defined as something consisting of mutually related elements and primitives, sometimes called *texels* [1]. Due to its wide variability, it is not simple to give a precise definition.

In this work, we present an approach to texture classification based on the description given by the estimation of the orientation in the points within a textured region. Therefore, we must first extract a value for the orientation and magnitude of the gradient in every point. From these estimations, we build an orientation histogram for each texture, which represents the distribution of the orientations. From the analysis of the Fourier coefficients of the histograms, we can measure the similarity of the textures. The distribution of orientations has been previously used in [2] for the discrimination between city and suburb photos according to the presence or absence of dominant orientations. Other works have shown the results of different filters used in texture classification when

applied to a certain texture benchmark set [3] and the evaluation of dissimilarity measures for color and texture [4]. A complete analysis on texture-related problems and applications, considering aspects like texture classification, segmentation or synthesis is shown in [5].

The paper has been structured as follows: Section 2 shows how the orientation of the edges can be estimated from the outputs of a set of filters. In Sect. 3, these estimations are used to build orientation histograms which describe the textures in terms of quantitative edge orientation distribution and the representation of the textures through these orientation histograms allows classifying them. Section 4 shows how darkening, lightening and inverting the images affect the classification, which proves robust under these transformations. Finally, Sect. 5 shows some conclusions about this work.

## 2. Edge Orientation Estimation

From Newton filters [6][7], we have developed a set of filters which preserve their convenient properties, but which also avoid some of the undesirable phenomena by providing them with rotational invariance and non-null weights in all positions. The weights of the eight filters and the orientations they react to are shown in Table 1.

The output of these filters is independent of the particular gray value of the image border, i.e.  $F_k$  is invariant under a gray level translation like  $I \rightarrow I + C$ , where  $I$  is the gray value of the image and  $C$  is any constant. This property is very important because the relevant information is provided by the difference between neighbors, rather than the magnitude of the image gray value.

The output of these eight filters for a  $\pi/2$  oriented edge of magnitude 1 is  $(0, 5, 8, 5, 0, -4, -4, -4)$ . If we increase or decrease the orientation in a multiple of  $\pi/4$ , the output is only cyclically shifted, but the values and their order are not altered. Figure 1 shows the outputs of the eight filters for a circle.

|                                                                        |                                                                        |
|------------------------------------------------------------------------|------------------------------------------------------------------------|
| $\begin{bmatrix} 1 & 1 & -2 \\ 2 & 2 & -4 \\ 1 & 1 & -2 \end{bmatrix}$ | $\begin{bmatrix} 1 & -2 & -4 \\ 1 & 2 & -2 \\ 2 & 1 & 1 \end{bmatrix}$ |
| $F_0 : 0$                                                              | $F_1 : \pi/4$                                                          |
| $\begin{bmatrix} -2 & -4 & -2 \\ 1 & 2 & 1 \\ 1 & 2 & 1 \end{bmatrix}$ | $\begin{bmatrix} -4 & -2 & 1 \\ -2 & 2 & 1 \\ 1 & 1 & 2 \end{bmatrix}$ |
| $F_2 : \pi/2$                                                          | $F_3 : 3\pi/4$                                                         |
| $\begin{bmatrix} -2 & 1 & 1 \\ -4 & 2 & 2 \\ -2 & 1 & 1 \end{bmatrix}$ | $\begin{bmatrix} 1 & 1 & 2 \\ -2 & 2 & 1 \\ -4 & -2 & 1 \end{bmatrix}$ |
| $F_4 : \pi$                                                            | $F_5 : 5\pi/4$                                                         |
| $\begin{bmatrix} 1 & 2 & 1 \\ 1 & 2 & 1 \\ -2 & -4 & -2 \end{bmatrix}$ | $\begin{bmatrix} 2 & 1 & 1 \\ 1 & 2 & -2 \\ 1 & -2 & -4 \end{bmatrix}$ |
| $F_6 : 3\pi/2$                                                         | $F_7 : 7\pi/4$                                                         |

Table 1. Modified Newton filters and corresponding orientation

When the real orientation does not correspond to one of these directions, we can estimate it by interpolating the higher value with its two neighbors, which provides an accurate estimation of edge orientation. A quadratic function is built to interpolate these three values and its maximum is used as the estimated orientation, as shown in (1), where  $i$  is the index of the filter with the highest output,  $F_i$ , and positions  $i - 1$  and  $i + 1$  are calculated modulo 8.

$$x_{\max} = \left( \frac{4F_i - 3F_{i-1} - F_{i+1}}{2[F_i - F_{i-1} - F_{i+1}]} + i - 1 \right) \frac{\pi}{4} \quad (1)$$

By correlating the ideal pattern with the real one, we can determine how perfect the border is. As the change from one side of the border to the other one may be larger than 1, it is necessary to normalize the output. Thus, the main advantage of this kind of filters is not the location of edges, but their classification according to their orientation and the invariance under rotations and illumination changes. Similar filters have been proposed by Prewitt, Sobel, Robinson or Kirsch [1], but they do not fit our needs as the modified Newton filters do.

### 3. Orientation-Based Texture Classification

The filters described in the previous section allow estimating the orientation of the gradient in a certain

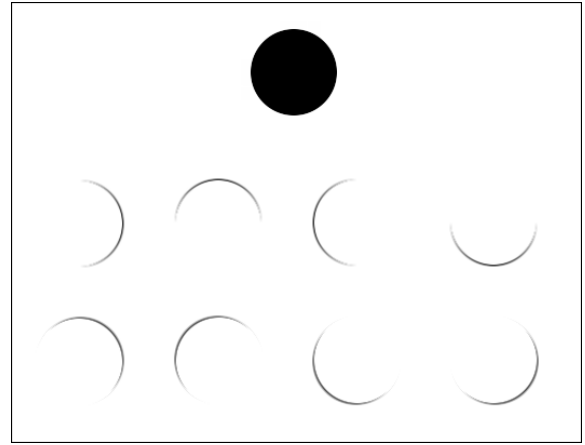


Figure 1. Positive outputs of the modified Newton filters for the circle above (the higher the output value, the darker it has been represented)

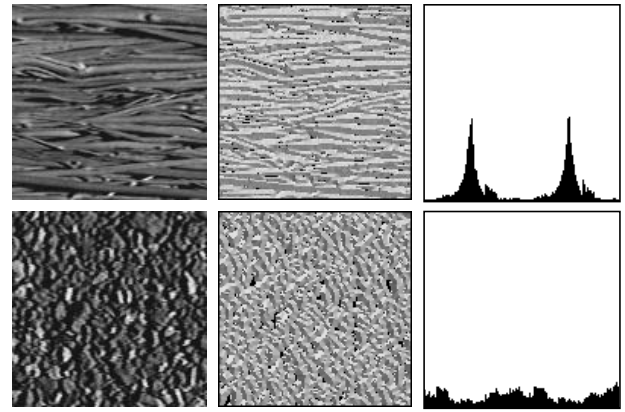


Figure 2. Texture examples and corresponding orientation maps and orientation histograms

pixel. Similarly, the values for the eight main orientations can be used to estimate the magnitude of the gradient. The interpolation of the outputs of the filters will provide us with a value for the orientation of the gradient in every point as well as an estimation of its magnitude. With these estimations, we build a histogram for the orientations by adding the magnitude of the gradients of the points where the edges present the same orientation. Figure 2 shows an example of two textures and their corresponding orientation histograms which can be used to compare these textures with others.

Using (1), the maximum value  $o_{j,k}$ , which esti-

mates the orientation in point  $(j, k)$ , is given by:

$$o_{j,k} = \text{round} \left( \frac{\left( \frac{4F_i - 3F_{i-1} - F_{i+1}}{2[2F_i - F_{i-1} - F_{i+1}]} \frac{\pi}{4} + \frac{\pi(i-1)}{4} \right) L}{2\pi} \right) \quad (2)$$

In order to adjust it to a discrete signal consisting of  $L$  equidistant values, we have rounded the values. For the magnitude, we use this orientation and substitute it in the polynomial:

$$\begin{aligned} (\nabla I)_{j,k} &= F_{i-1} \quad (3) \\ &+ \frac{8F_i - 2F_{i+1} - 6F_{i-1}}{\pi} \left( o_{j,k} - \frac{\pi(i-1)}{4} \right) \\ &+ \frac{8F_{i+1} - 16F_i + 8F_{i-1}}{\pi^2} \\ &\left( o_{j,k} - \frac{\pi(i-1)}{4} \right)^2 \end{aligned}$$

The values of the histogram  $h_i$  are given by the following expression, where  $(\nabla I)_{j,k}$  and  $o_{j,k}$  are the magnitude and the orientation extracted for point  $(j, k)$ . For normalization purposes, the global weight of all positions in the histogram is set to 1, thus dividing each resulting component of the histogram by the sum of all of them:

$$h_i = \sum_{\substack{j,k \\ o_{j,k}=i}} (\nabla I)_{j,k} \quad (4)$$

$$h'_i = \frac{h_i}{\sum_{j=0}^{L-1} h_j} \quad (5)$$

In order to relate two textures, an energy function is built, in which the Fourier coefficients of both histograms are compared. We must achieve rotational invariance, in the sense that the result must not be affected if the textures are rotated. A change in the orientation of a texture will only cause a cyclical shift in the histogram. For this reason, the Fourier coefficients are modified as follows: let  $f_n$  and  $g_n$  be the orientation histograms of length  $L$  corresponding to the same texture but shifted  $a$  positions, i.e. the texture has been rotated an angle  $\theta = 2\pi a/L$ , and let  $f_k$  and  $g_k$  be the  $k^{\text{th}}$  Fourier coefficients of these histograms, then:

$$f_k = g_k e^{-i \frac{2\pi ka}{L}} \quad (6)$$

Thus, a measure of how similar the coefficients of both textures are is given by:

$$E(a) = \sum_{k=1}^{\frac{L}{2}} \left( f_k - g_k e^{-i \frac{2\pi ka}{L}} \right) \left( f_k - g_k e^{-i \frac{2\pi ka}{L}} \right)^* \quad (7)$$

The fact that the number of discrete orientations used for the histograms is constant and the normalization of the weights make the lengths of the signals and the total weight equal in both textures. Consequently, a change in the size of the region where the texture is analyzed will not cause the generation of a different distribution. Due to the fact that the higher frequencies are more noise-sensitive than the lower ones, a monotonic decreasing weighting function  $w(\cdot)$  can be used to emphasize the discrimination, thus obtaining the following expression, in which the first terms have a more important contribution than the last ones:

$$E(a) = \sum_{k=1}^{\frac{L}{2}} w \left( \frac{2k}{L} \right) \left( f_k - g_k e^{-i \frac{2\pi ka}{L}} \right) \left( f_k - g_k e^{-i \frac{2\pi ka}{L}} \right)^* \quad (8)$$

We have tested different linear, quadratic and exponential weighting functions and the best results were obtained for the exponential functions, more precisely, using  $e^{-10x}$  (see fig. 3).

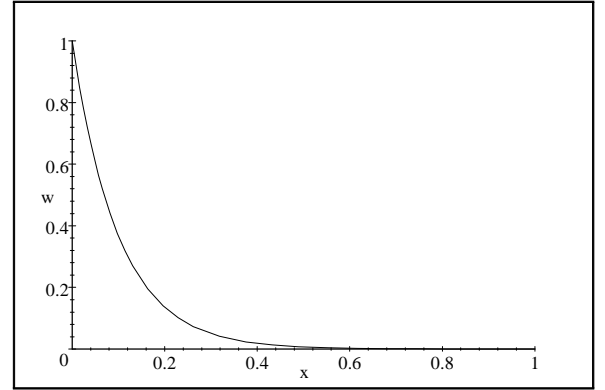


Figure 3. Exponential weighting function  $e^{-sx}$  for  $s = 10$

To test this technique, we have used a set of textures contained in a database, which is shown in fig. 4. This database has been made publicly available for research purposes by Columbia and Utrecht Universities, Columbia-Utrecht Reflectance and Texture Database [8]. We work with grayscale images and thus, a single histogram is used to represent the orientations of the edges in light intensity. If we were working with color images, a three subchannel mechanism could be used when hue, and not only intensity, is relevant for texture identification. Using the techniques described above, a certain texture is compared with all those in the database and the most similar ones are selected. The similarity between two textures is given by the

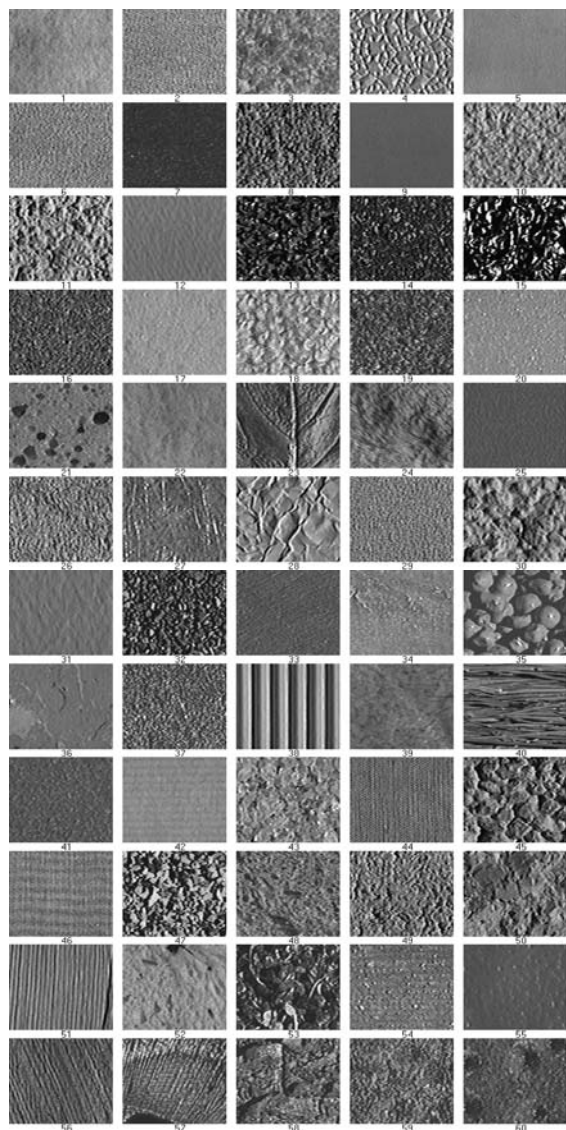


Figure 4. Database textures

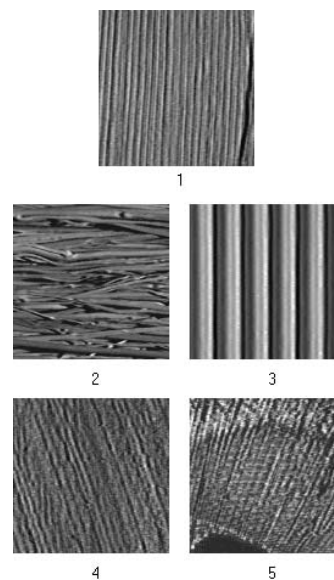


Figure 5. Results of searching for similar textures for texture 51

| order | txt. number | wtd. energy |
|-------|-------------|-------------|
| 1     | 51          | 0.00        |
| 2     | 40          | 16.03       |
| 3     | 38          | 49.21       |
| 4     | 56          | 118.39      |
| 5     | 57          | 157.10      |

Table 2. Lowest energies for texture 51

energy obtained when comparing their orientation histograms.

In fig. 5 and fig. 6, we show some results of the application of the technique explained above. From the image database containing 60 textures of different natures, but visually difficult to classify, one is selected and the five best comparisons are shown. Of course, as the selected image belongs to the set, the best match corresponds to itself, and the energy factor is 0.

| order | txt. number | wtd. energy |
|-------|-------------|-------------|
| 1     | 11          | 0.00        |
| 2     | 30          | 0.59        |
| 3     | 49          | 0.61        |
| 4     | 10          | 1.20        |
| 5     | 26          | 1.62        |

Table 3. Lowest energies for texture 11

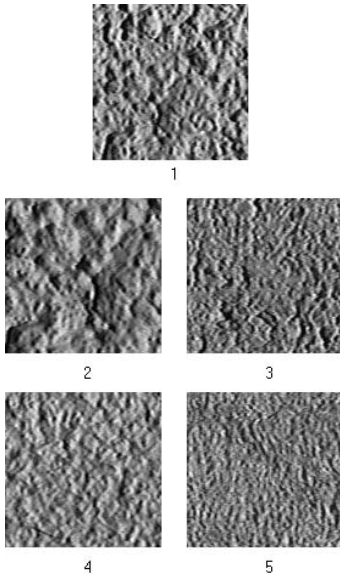


Figure 6. Results of searching for similar textures for texture 11

#### 4. Robustness of Texture Classification under Darkening, Lightening and Inversion

The following examples show how darkening, lightening and inverting a pattern affect the results when calculating the energy which measures the similarity between two textures. This will allow us to test the robustness of our method when some kinds of transformations are performed in the input signal.

Darkening is obtained by multiplying the original values by a constant, lower than 1. For lightening, the same process is executed, but in this case we use a constant higher than 1. Finally, inversion is obtained by subtracting the input values from 255, which is the maximum value.

As observed in fig. 7 and in Table 4, when a texture is darkened, the resulting energy is very low. The use of integer values in intensity representation forces us to round the values once they have been reduced, generating small differences in gradient values.

Figure 8 and Table 5 show similar consequences when the textures are lightened. In this case, the overflow in light intensity values for the most bright points due to the increase they undergo, which forces us to truncate the values which exceed the maximum, causes a higher difference.

Finally, fig. 9 and Table 6 show the results when a texture has been inverted. As observed, the values obtained are very low and the patterns can be considered as the same texture.

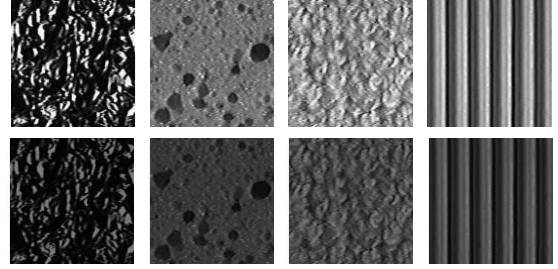


Figure 7. Textures 15, 18, 21 and 38 before and after darkening

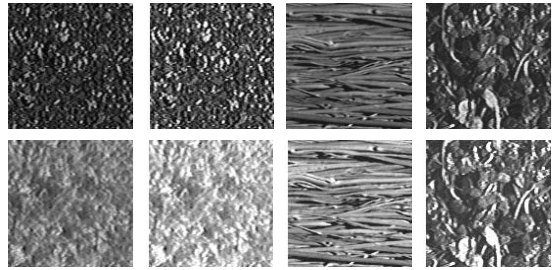


Figure 8. Textures 3, 14, 40 and 53 before and after lightening

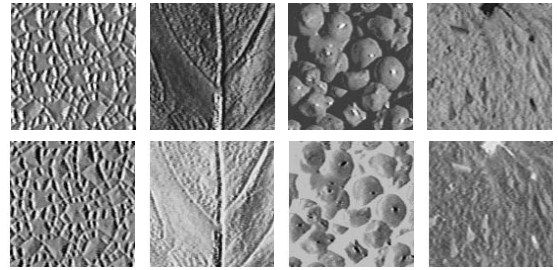


Figure 9. Textures 4, 23, 35 and 52 before and after inversion

| comparison | wtd. energy |
|------------|-------------|
| 15-drk.15  | 0.0083      |
| 18-drk.18  | 0.0050      |
| 21-drk.21  | 0.0129      |
| 38-drk.38  | 0.0145      |

Table 4. Comparison of some textures with their darkened versions

| comparison | wtd. energy |
|------------|-------------|
| 03-lgt.03  | 0.0374      |
| 14-lgt.14  | 0.0117      |
| 40-lgt.40  | 0.0052      |
| 53-lgt.53  | 0.0757      |

Table 5. Comparison of some textures with their lightened versions

| comparison | wtd. energy |
|------------|-------------|
| 04-inv.04  | 0.2567      |
| 23-inv.23  | 0.4859      |
| 35-inv.35  | 0.6009      |
| 52-inv.52  | 0.4927      |

Table 6. Comparison of some textures with their inverted versions

## 5. Conclusion

In this work, we have presented a new approach to texture classification. By using the modified Newton filters, we have obtained an estimation of the orientation of the edges in every point of the textures. The extraction of orientation histograms to describe the distribution of the orientations across a textured region permits us to perform a comparison of the textures according to the quantitative and relative distribution of the different orientations.

The analysis of the Fourier coefficients and certain normalization processes which have been included allows a satisfactory classification, including size and rotational invariance. The introduction of a weighting function for the different Fourier coefficients has improved the discrimination. Furthermore, we have tested how our method reacts when the textures are darkened, lightened or when their grayscale levels are inverted, obtaining very satisfactory results.

The quite promising numerical results obtained in the tests which have been implemented confirm the usefulness of this technique for the comparison of the images, since they endow us with a very robust discrimination criterion.

## References

[1] M. Sonka, V. Hlavac, and R. Boyle, *Image processing, analysis, and machine vision*, PWS-ITP, 1999.

[2] M.M. Gorkani and R.W. Picard, Texture orientation for sorting photos "at a glance", *proceedings of IEEE conference on pattern recognition I*, 1995, 459-464.

[3] T. Randen and J.H. Husøy, Filtering for texture classification: a comparative study, *IEEE Transactions on Pattern Analysis and Machine Intelligence* 21(4), 1999, 291-310.

[4] J. Puzicha, J.M. Buhmann, Y. Rubner and C. Tomasi, Empirical evaluation of dissimilarity measures for color and texture, *proceedings of the IEEE International Conference on Computer Vision (ICCV'99)*, 1999, 1165-1173.

[5] M. Tuceryan and A.K. Jain, Texture Analysis, in C.H. Chen, L.F. Pau, P.S.P. Wang, editors, *The Handbook of Pattern Recognition and Computer Vision*, 2nd edition, World Scientific Publishing Co., 1998.

[6] R. Moreno-Díaz jr., *Computación paralela y distribuida: relación estructura-función en retinas*, Tesis Doctoral, 1993.

[7] M. Alemán-Flores, L. Álvarez-León and R. Moreno-Díaz jr., Modified Newton filters for edge orientation estimation, shape representation and motion analysis, *Cuadernos del Instituto Universitario de Ciencias y Tecnologías Cibernéticas*, Universidad de Las Palmas de Gran Canaria 17, 2001, 1-30.

[8] Columbia University and Utrecht University. *Columbia-Utrecht Reflectance and Texture Database*. <http://www.cs.columbia.edu/CAVE/curet/>.